Ultracapacitor Energy Storage Systems based on Dynamic Setting and Coordinated Control for Urban Trains

Xin WANG [*] **Yingbing LUO** [*] **Bin QIN** [†][*] **Junming PENG** [*]
Yu ZHOU [*] **Zhongcan SUN** [*]

[*] *College of Electrical & Information Engineering, Hunan University of Technology, Zhuzhou, Hunan, 412007 China.* [†] *Corresponding author: e-mail: qinbin99p@163.com*

Abstract: The supply voltage of traction systems fluctuates frequently due to acceleration and braking during urban rail train running process. In order to achieve better performance for ultracapacitor energy storage systems, a bilateral ultracapacitor energy storage system structure is adopted, and a method based on dynamic setting and coordination is proposed, in which the charge and discharge voltage thresholds of ultracapacitors are dynamically set and the energy flows are coordinated controlled between the bilateral ultracapacitor energy storage systems. The simulation results show that the proposed control strategy can achieve good energy-saving effect and stabilize the traction network voltage under the premise of balanced use of the ultracapacitor energy storage systems.

Keywords: Urban rail train, Ultracapacitor, Dynamic setting, Coordinated control

1. INTRODUCTION

In recent years, the ultracapacitor as a new energy storage device has attracted increasing attention and been gradually applied in rail transit systems. (Zhu et al., 2018). It has many advantages such as high power densities, fast charge-discharge speed and so on. Its high-quality performance matches the operational characteristics of urban rail trains (Wang et al., 2014). In (Battistelli et al., 2012), the maximum recovery effect was achieved by real-time estimating maximum average power from a unilateral power supply system model. In (Ciccarelli et al., 2014), a new control strategy considering train speed and acceleration was proposed to ensure the charge state of each station. However, it is necessary to obtain real-time train information in real applications which increases the difficulty of implementation. In general, substations and trains are considered as urban rail transit models, while the problems of dc-link voltage fluctuations and dc-link voltage instability in the dc traction systems are ignored at the same time (Naseri et all., 2020). The fluctuation of no-load voltage, the change of the headway distance, and the braking resistance characteristics of trains affect the charge and discharge voltage threshold setting and the energy saving.

A single energy storage system structure is usually adopted in urban rail operation zones (Tang et al., 2017), which have a good effect on stabilizing traction grid voltage and saving energy, but line loss in the unilateral energy storage system is large. How to set the charge and discharge voltage thresholds of ultracapacitors according to the actual working conditions and real-time data is particularly important to exert good system energy saving effect (Wang et al., 2015). In this paper, an energy management control s-

trategy for bilateral ultra-capacitor energy storage systems is proposed based on the traditional control strategies, in which the charge-discharge thresholds are dynamically set to achieve energy management coordination by tracking the train real-time running distance.

The remaining parts of this paper are organized as follows: section 2 describes the improved control strategy in detail. In section 3, the experiments to validate the proposed control strategy are discussed. Finally, a conclusion is given in section 4.

2. THEORY AND METHODS

2.1 Traction Power Supply Structure of Bilateral Ultracapacitor Energy Storage System

The proposed traction power supply structure of an urban rail train with bilateral ultracapacitor energy storage systems mainly consists of four parts: traction substations, DC traction gridsFig4, an urban rail train with PMSM and two ultracapacitor energy storage systems, as shown in Fig. 1.
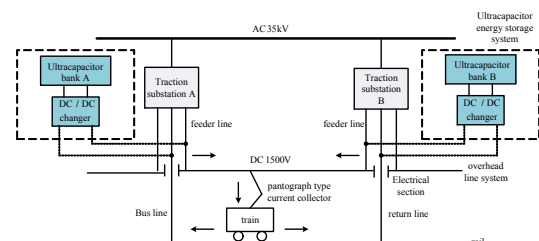

Fig. 1. Traction power supply structure with bilateral ultracapacitor energy storage systems

The traditional bilateral energy storage systems are independent of each other and the coordinated control strategies for energy flows between bilateral energy storage systems are not considered, leading to energy saving and maximum utilization unguaranteed. Therefore, in this paper, a focus is on the coordination and optimal control of charge and discharge energy flows of bilateral energy storage systems in the same power supply section.

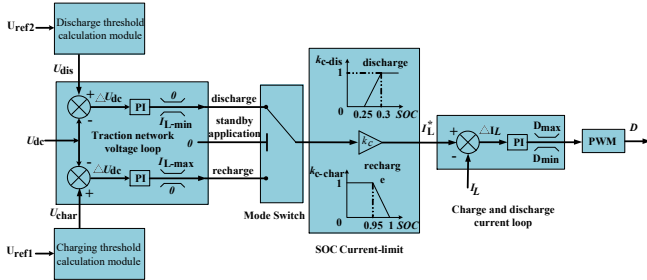### 2.2 Coordinated control of traction network voltage

Fig. 2. Control diagram of energy storage systems based on dynamic regulation and coordinated control

The train running state is reflected directly based on dc traction net voltage fluctuation in the double closed-loop control structure of traditional energy storage systems and the ultracapacitor energy storage system working mode is determined by setting the charge-discharge voltage thresholds and detecting traction net voltage. On the basis of traditional control strategies, an improved energy management strategy for bilateral energy storage systems with dynamic setting and coordinated control is proposed. The control block diagram is shown in Fig. 2. It is mainly divided into the following parts: energy storage system switching mode, current-voltage dual-loop cascade control module, charge and discharge threshold calculation module and SOC current limit module.

2.3 Energy Storage System Switching Mode

The bidirectional dc/dc converters can achieve bidirectional energy transfer among different voltage levels by reasonably controlling the conduction ratio of power electronic switching devices. A half-bridge non-isolated BDC topology is shown in Fig. 3. (Ronanki et al., 2017). Functionally,
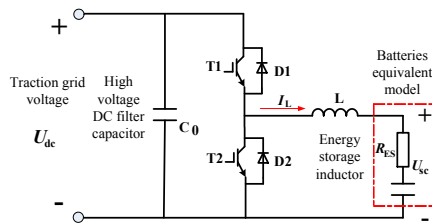

Fig. 3. Half-bridge non-isolated BDC

the BDC is actually an inverse parallel combination of Boost-Buck type chopper circuits. It can be switched among Boost, standby and Buck working modes to realize BDC power bidirectional transmission and input/output two-quadrant operation by controlling the conduction ratio of two switching tubes T1 and T2. In the case of train

traction and acceleration, the BDC works in the Boost mode, and the energy storage systems discharge energy to the traction net. When the train runs in coasting, the energy storage systems are in standby mode. In the case of train braking deceleration, the BDC works in the Buck mode, and the energy storage systems recover the energy fed back from the train braking to the traction net. In order to prevent the breakdown and damage of switching devices caused by too high charge voltage of energy storage systems, and the misoperation accidents, the energy storage systems are set with the ban mode. The working mode switching principle for bilateral energy storage systems are shown in Fig. 4. A key parameter in ultracapacitor energy
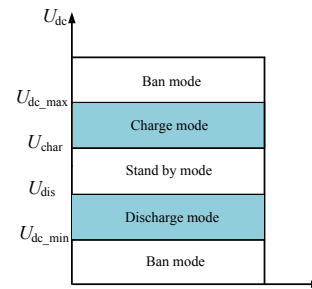

Fig. 4. Working mode switching schematic diagram

storage systems is SOC (State of Charge, SOC) calculation and compensation. It is used to indicate the charge state of energy storage systems (battery, Ultracapacitor, etc.) and related to the ultracapacitor voltage. Its value ranges from 0 to 1.

Since the capacitance values change continuously during the ultracapacitor charge-discharge processes, according to the equation $\Delta U = \Delta Q/C$, the dynamic capacitance correction factor Cu must be considered on the basis of the electromotive force if the SOC information, that is, the charge quantity Q, is obtained accurately.

According to the real-time electromotive force, average discharge current and temperature of the ultracapacitors, the normalized SOC estimation error of the electromotive force is corrected by solving the dynamic capacitance correction factor under full working condition prediction model.

C_u is calculated in real-time during discharge process with the change of electromotive force by an SVM-based C_u model. (Wei et al., 2017), and the SOC estimated value after dynamic capacitance correction is calculated according to equation (1). The maximum error is reduced to 3.4%, 2.8% and 2.5%, respectively under $10°C$, $25°C$ and $40°C$ random current conditions

$$SOC = \frac{U(t) - U_{sc\min}}{U_{sc\max} - U_{sc\min}}C_u \qquad (1)$$

Where $U(t)$ is the real-time electromotive force of ultracapacitors, U_{scmax} and U_{scmin} are the maximum and minimum discharge voltage before normalization, respectively. C_u is the correction factor. the SOC working range of ultracapacitors is generally set to $0.25 \sim 0.95$ considering a certain safety margin.

2.4 Current-voltage dual-loop cascade control

Combining the above requirements, a current-voltage dual-loop cascade control is adopted. The outer control ring is the dc traction network voltage ring, and the inner control ring is the ultracapacitor current ring. The magnitude and direction of charge-discharge current are determined according to the error between actual values and given values, A BDC dual-loop cascade control block diagram is shown in Fig. 5. The state space averaging
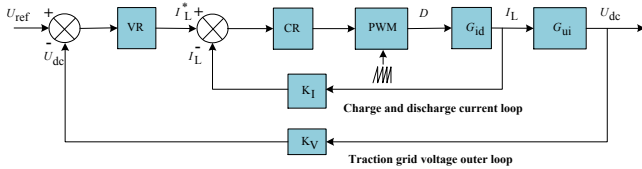
Fig. 5. BDC dual-loop cascade block diagram

method is used to perform BDC mathematical modeling analysis in Buck and Boost modes, respectively. In Fig. 5, G_{id} and G_{ui} are the open-loop small-signal transfer functions of duty-cycle D to inductance current I_L and inductance current I_L to traction grid voltage U_{dc}, respectively. Their representation is shown in equation (2) (Yang et al., 2020),

$$\begin{cases} G_{i_L d}(s) = \dfrac{U_{dc}C_{sc}s}{LC_{sc}s^2 + R_{ES}C_{sc}s + 1} \\ G_{u_{dc}i_L}(s) = \dfrac{LC_{sc}s^2 + R_{ES}C_{sc}s + 1}{DC_{sc}s} \end{cases} \quad (2)$$

It can be seen that the BDC is a second-order oscillation circuit with two controlled state variables: the ultracapacitor set terminal voltage U_{sc} and the energy storage inductance current I_L.

The difference between the actual traction grid voltage and the given charge-discharge voltage threshold is adjusted by a PI outer loop to obtain charge-discharge reference current I_L^*. The difference between I_L^* and the actual charge-discharge feedback current I_L is regulated by a current PI inner loop, and the duty-cycle D that drives the BDC switching devices is obtained through PWM control.

2.5 Charge and discharge dynamic threshold calculation module

The charge threshold of the traction net voltage outer loop U_{char} is expressed by equation (3). The SOC value is the square ratio of the terminal voltage of the ultracapacitor set to the rated voltage. The SOC range is generally set between 0.25 and 1. U_{ref1} is the given reference constant charge threshold. L is the distance between the train real-time position and the substation (or energy storage system) in the power supply section. k_l and k_{10} are the control parameters.

When the storage capacity of energy storage systems is large, SOC ≤ 0.95, the charge thresholds of bilateral energy storage systems are dynamically set by tracking the train real-time running distance in the power supply section and SOC values, namely, the lower charge thresholds and the corresponding larger charge current are got, and more braking energy feedback is taken on by wayside energy storage systems when the train is closer to them. When

0.95 < SOC < 1, The overall charge thresholds of energy storage systems increase with the increase of SOC values, and the corresponding charge current gradually decreases. The energy flows of bilateral energy storage systems is coordinated controlled by tracking train real-time running distance and SOC values, namely, On the premise of fully and effectively feeding back the train braking energy, the charge current is coordinated controlled by the energy storage systems in each station based on their own capacity and minimum line loss, and the charge thresholds of bilateral energy storage systems are negatively correlated with the charge current.

$$U_{char} = \begin{cases} U_{ref1} + k_1 l, SOC \le 0.95 \\ U_{ref1} + k_1 l_1 (SOC - 0.95), 0.95 < SOC < 1 \end{cases} \quad (3)$$

Similarly, the discharge threshold of the traction net voltage outer loop U_{dis} is expressed by equation (4). U_{ref2} is the given reference constant discharge threshold, and k_2 and k_{20} are the control parameters.

$$U_{dis} = \begin{cases} U_{ref2} + k_2 l, SOC \ge 0.3 \\ U_{ref2} + k_2 l + k_{20}(0.3 - SOC), 0 < SOC < 0.3 \end{cases} \quad (4)$$

2.6 SOC current limit module

$$k_{c-chatr} = \begin{cases} 1, SOC \le 0.95 \\ 20 \times (1 - SOC), 0.95 < SOC < 1 \\ 0, SOC = 1 \end{cases} \quad (5)$$
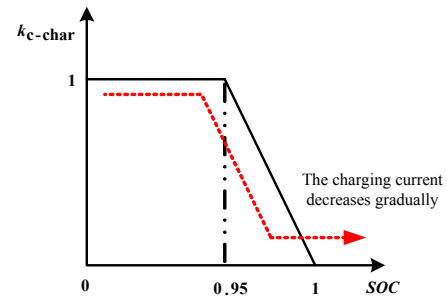
The functional relationship between SOC values and the

Fig. 6. Relationship between SOC values and k_{c-char} in charge mode

current limit link k_{c-char} in the charge mode is shown in equation (5) and Fig. 6, respectively. Also, the functional relationship between SOC values and the current limit link k_{c-dis} in the discharge mode is shown in equation (6) and Fig. 7, respectively.

$$k_{c-dis} = \begin{cases} 0, SOC \le 0.25 \\ 20 \times (SOC - 0.25), 0.25 < SOC < 0.3 \\ 1, SOC \ge 0.3 \end{cases} \quad (6)$$

The charge and discharge current are controlled by SOC values when the ultracapacitor energy storage systems operate in charge and discharge modes normally. Besides, the SOC values of ultracapacitor set gradually reduce the charge current after reaching upper limit in the charge mode, thus avoiding the ultracapacitor set out of operation in the form of rapid removal of large current near full load. Quick large current removal should be also avoided after discharge to a certain depth in the discharge mode.
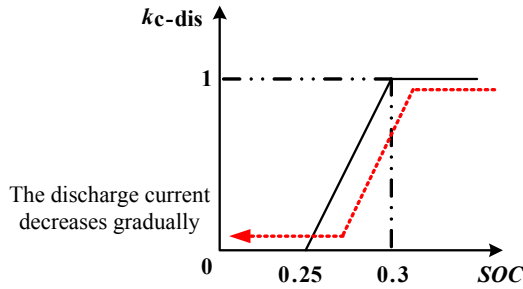
Fig. 7. Relationship between SOC values and k_{c-dis} in discharge mode

3. RESULTS AND DISCUSSION

3.1 Simulation Parameters

Table 1. Control parameters of bilateral energy storage systems

Energy storing device	Charge mode	Discharge mode
Traction substation A	$k_1 = 2$ $k_{10} = 1000$	$k_2 = 2$ $k_{20} = 1000$
Traction substation B	$k_1 = 10$ $k_{10} = 2000$	$k_2 = 0.5$ $k_{20} = 2000$

Here, the given reference constant charge and discharge thresholds are set as: $U_{ref1} = 1600V$, $U_{ref2} = 1300V$; the control parameters k_l and k_{10}, as well as k_2 and k_{20} are got according to the multiple experiment results, which are shown in Table 1. Simulation time, traction acceleration time and train braking deceleration time are set as 2s, 0.48s, 1.5s, respectively. The functional relationship between the train real-time running distance L and time t in a power supply section is shown in Fig. 8. The permanent

Table 2. Ultracapacitor parameters

Energy storage element	Single capacity	Number of series	Number of parallel groups
Ultracapacitor	69.63F	370	13

magnet synchronous traction motor is selected and its parameters are: stator resistance $R_s = 0.285\Omega$, equivalent d, q-axis inductance $L_d = L_q = 2.5mH$, pole pair $p_n = 4$, rotor permanent magnet flux linkage $\Psi_f = 0.75Wb$. The specific parameters of the Ultracapacitor monomer are shown in Table 2. Suppose a train moves from station A to
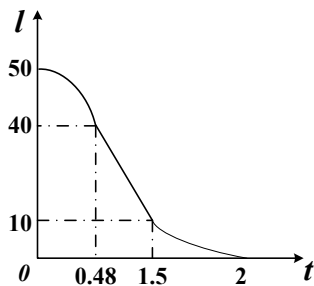

Fig. 8. Relationship between train distance and time

station B with traction acceleration, coasting and braking deceleration. According to the time ratio of 1:20, 0-0.48s,

train traction acceleration, is considered as uniformly accelerated motion, 0.48-1.5s, train coasting, is considered as uniform velocity motion, 1.5-2s, train braking deceleration, is considered as uniformly decelerated motion. The functional relationship between L and time t is expressed in equation (7).

$$l = \begin{cases} -43.4t^2 + 50, 0 \le t \le 0.48 \\ -29.41t + 54.12, 0.48 < t \le 1.5 \\ 40(t-2)^2, 1.5 < t \le 2 \end{cases} \quad (7)$$

3.2 Simulation Result Analysis

The traction net voltage comparison of the urban rail energy storage systems with different control strategies is shown in Fig. 9. The traction network voltage is fluctuated greatly if the energy storage systems are not used during train braking and starting processes. n the case of setting
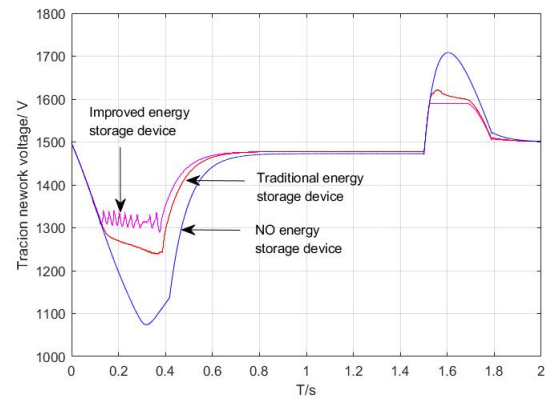

Fig. 9. Traction net voltage comparison with different control strategies

the same charge and discharge thresholds, the traction net voltage is stabilized at about 1250V in train traction acceleration and 1620V in braking deceleration with the traditional energy storage system control strategy. There is a gap between the actual traction net voltage and the given target of 1300-1600v, and the fluctuation range is large. While the voltage stabilizing and energy saving effects of the traction net are significantly improved with the improved control strategy. The traction net voltage is stabilized above 1300V in train traction acceleration and below 1600V in braking deceleration. In addition, the traction net voltage is more stable during the voltage stabilizing process, and the braking energy utilization is also greatly improved. The energy flows between the energy storage systems and the traction net is more efficient and energy-saving. The initial terminal voltage and maximum working voltage of the ultracapacitors are set as 500V. The terminal voltage change of bilateral energy storage systems without SOC limit during whole train operating process is shown in Fig. 10 and it is compared with that of a single energy storage system with the traditional control strategy. The terminal voltage of the single energy storage system varies greatly in the process of charge and discharge with the traditional control strategy, while the terminal voltage variation range of bilateral energy storage systems is reduced with the improved control strategy.
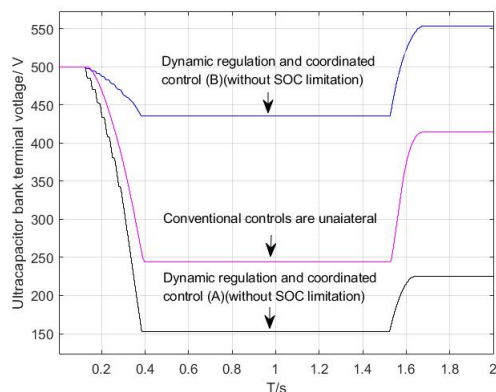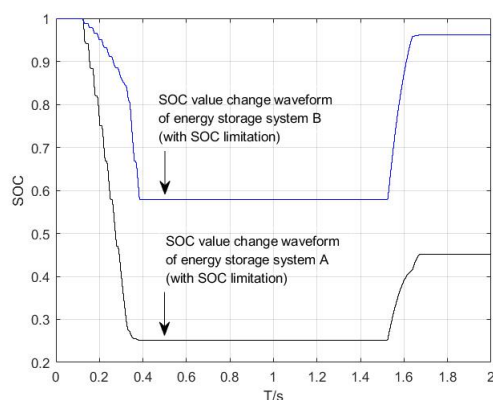
Fig. 10. Ultracapacitor bank terminal voltage

Fig. 11. SOC change waveform with SOC limit

In train traction acceleration, the energy storage device A close to the train real-time position is mainly responsible for voltage stabilization, and the terminal voltage variation range is greater than that of energy storage device B. The wayside energy storage system B far from the train has a small discharge current, and the terminal voltage only drops by about 60V. In train braking deceleration, the energy storage device B close to the train real-time position undertakes most of braking energy utilization, and the terminal voltage variation range is greater than that of energy storage device A. The wayside energy storage system A far from the train has a small charge current, and the terminal voltage only rises by about 70V. The charge and discharge of bilateral energy storage systems is dynamically coordinated with the change of train real-time running distance, thus the line loss in the charge-discharge process being reduced.

The SOC values change with time in the case of SOC limit is shown in Fig. 11 The discharge depth is more than 0.25 in the discharge mode, and the charge depth does not exceed the maximum working voltage in the charge mode.

The change of discharge thresholds of bilateral energy storage systems with time is shown in Fig. 12.i) The traction net voltage is dropped due to train traction acceleration and the traction net is discharged by the bilateral energy storage systems at the same time. A higher discharge threshold, up to 1400V, is got by energy storage system A closer to the train and set dynamically with

the train real-time running distance. When the discharge depth of energy storage system A is close to the limit (SOC≥0.25), it is transferred to energy storage system B to undertake the main voltage stabilizing task. The discharge threshold of energy storage system B increases suddenly from 1325V, and it is greater than that of energy storage system A. The change of charge thresholds
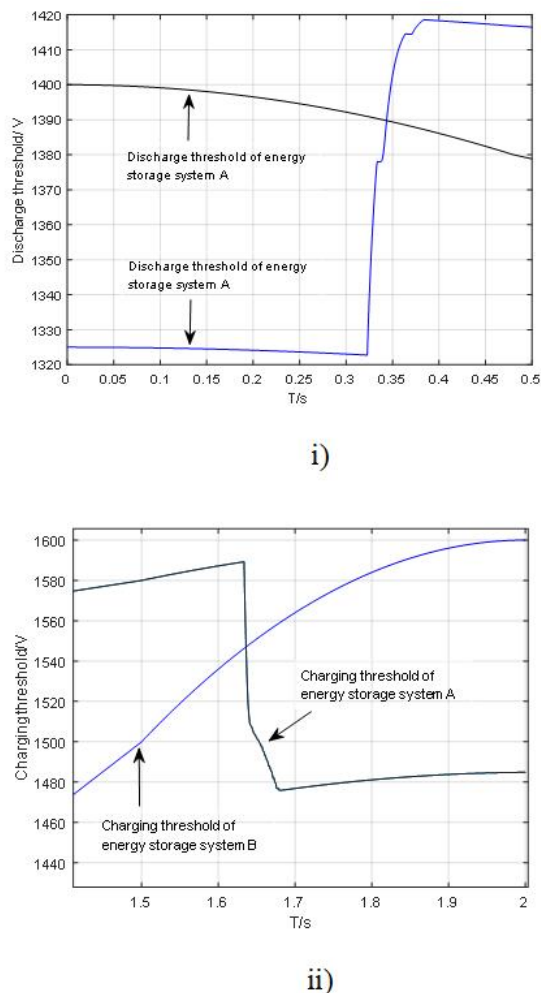

i)

ii)

Fig. 12. The charge threshold variation of bilateral energy storage systems i) discharge threshold, ii) charging threshold

of bilateral energy storage systems with time is shown in Fig. 12.ii) The traction net voltage is risen due to train braking deceleration. Most of braking energy is utilized by the wayside energy storage system B close to the train during early charge stage and it has a low charge threshold, reaching as low as 1500V. When the charge depth of energy storage system B is close to the limit (0.95 < SOC < 1), it is transferred to energy storage system A to undertake most of braking energy and the discharge threshold decreases, so dynamic setting charge and discharge thresholds and coordinated control of energy flows of bilateral energy storage systems are realized. The terminal voltage of bilateral energy storage systems changes with time with SOC value limit based on dynamic setting and coordinated control is shown in Fig. 12. According to the terminal voltage change of each energy storage system, under the condition of the
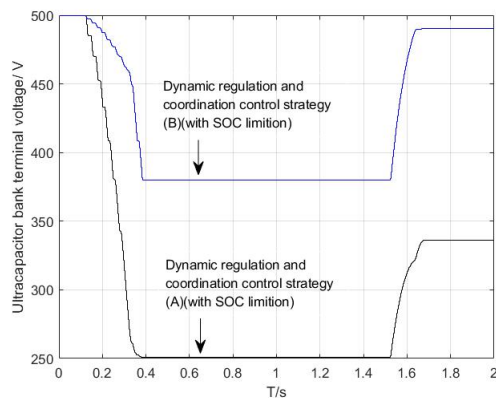
Fig. 13. Terminal voltage variation of bilateral energy storage systems based on dynamic setting and coordinated control

charge and discharge depth (SOC value) limit, each energy storage system can work stably within the safe working voltage range, that is, the minimum working voltage is 250V, the maximum working voltage is 500V. The energy flows of bilateral energy storage systems are dynamic setting and coordinated controlled by tracking the train real-time running distance and the SOC values.

4. CONCLUSIONS

An improved energy storage system energy management strategy based on dynamic setting and coordinated control is proposed in this paper. The simulation results verify its effectiveness. The energy saving and voltage stabilizing effect of energy storage systems are improved. Also, the energy flows of energy storage systems installed in traction substations can be regulated dynamically and coordinated through tracking the train real-time running distance and SOC variation. The utilization degree of each energy storage system tends to be balanced and reasonable. However, the proposed strategy is only applied to a single train. It is necessary to further study the up train and down train together in the same power supply section in the future.

ACKNOWLEDGEMENTS

REFERENCES

[1].Battistelli, L., Fantauzzi, M., Iannuzzi, D. (2012). Energy management of electrified mass transit systems with Energy Storage devices[C]. International Symposium on Power Electronics, Electrical Drives, Automation and Motion, 2012: 1172-1177.

[2].Ciccarelli, F., Del Pizzo, A., Iannuzzi, D. (2014). Improvement of Energy Efficiency in Light Railway Vehicles Based on Power Management Control of Wayside Lithium-Ion Capacitor Storage[J]. IEEE Transactions on Power Electronics, 2014, 29(1): 275-286.

[3].Naseri, F., Farjah, E., Kazemi, Z., Schaltz, E., Ghanbari, T., Schanen, J. (2020). "Dynamic Stabilization of DC Traction Systems Using a Supercapacitor-Based Active Stabilizer With Model Predictive Control," in IEEE Transactions on Transportation Electrification, vol. 6, no. 1, pp. 228-240, March 2020.

[4].Ronanki, D., A. Singh, S,. S, Williamson, S. (2017). "Comprehensive Topological Overview of Rolling Stock Architectures and Recent Trends in Electric Railway Traction Systems," in IEEE Transactions on Transportation Electrification, vol. 3, no. 3, pp. 724-738, Sept. 2017.

[5].Tang, Lianfu., Wu, Lixin. (2017). "Research on the Integrated Braking Energy Recovery Strategy Based on Super-Capacitor Energy Storage," 2017 International Conference on Smart Grid and Electrical Automation (ICSGEA), Changsha, 2017, pp. 175-178.

[6].Wang, Wei., Cheng, Ming., Wang, Ya et al.(2014). "A Novel Energy Management Strategy of Onboard Supercapacitor for Subway Applications With Permanent-Magnet Traction System," in IEEE Transactions on Vehicular Technology, vol. 63, no. 6, pp. 2578-2588, July 2014.

[7].Wang, Junxing., Yang, Zhongping., Fei, Lin. (2015). "Thresholds modification strategy of wayside supercapacitor storage considering DC substation characteristics," IECON 2015 - 41st Annual Conference of the IEEE Industrial Electronics Society, Yokohama, 2015, pp. 002076-002081.

[8].Wei, Li., Zhang, Shibo., Yao, Yongtao., Miao, Xiaoli., Zhang, Jin., Weng, Huanming.(2017). SOC estimation of hybrid supercapacitor based on dynamic capacitance correction [J]. Chinese Journal of Electrical Engineering, 2017, 37 (17): 5188- 5197 + 5239.

[9].Yang, Zhongping., Zhu, Feiqin., Lin, Fei. (2020). "Deep-Reinforcement-Learning-Based Energy Management Strategy for Supercapacitor Energy Storage Systems in Urban Rail Transit," in IEEE Transactions on Intelligent Transportation Systems.

[10].Zhu, Feiqin., Yang, Zhongping., Xia, Huan., Fei, Lin. (2018). "Hierarchical Control and Full-Range Dynamic Performance Optimization of the Supercapacitor Energy Storage System in Urban Railway," in IEEE Transactions on Industrial Electronics, vol. 65, no. 8, pp. 6646-6656, Aug. 2018.